

**THE EFFECT OF ROOF SLOPE ON THE WIND
PRESSURE DISTRIBUTION OF A LOW-RISE
MONO-PITCH HOUSE USING CFD SIMULATION**

MUHAMMAD FAIZ BIN AHMAD JAWARI

**SCHOOL OF CIVIL ENGINEERING
UNIVERSITI SAINS MALAYSIA
2022**

**THE EFFECT OF ROOF SLOPE ON THE WIND PRESSURE
DISTRIBUTION OF A LOW-RISE MONO-PITCH HOUSE USING
CFD SIMULATION**

By

MUHAMMAD FAIZ BIN AHMAD JAWARI

This dissertation is submitted to

UNIVERSITI SAINS MALAYSIA

As partial fulfilment of requirement for the degree of

**BACHELOR OF ENGINEERING (HONS.)
(CIVIL ENGINEERING)**

School of Civil Engineering
Universiti Sains Malaysia

August 2022

ACKNOWLEDGEMENT

By the grace of Allah S.W.T., I have successfully completed my dissertation. Prior to anything else, I would want to convey my profound appreciation to my supervisor, Prof. Ir. Dr. Taksiah A. Majid, for the opportunity, supervision, devotion, courteous guidance, and support during the duration of this project. I would also want to thank Ir. Dr. Shaharudin Shah Zaini, my second supervisor, for his assistance and expertise. Without their excitement and interest in my study, it would not have been possible to complete this project. I would also want to thank Mrs. Junaidah Abdullah for her assistance in providing me with a wealth of knowledge, experience, and direction, as well as assisting me with the technical work.

Without my parents Ahmad Jawari Diman and Che Mah Awang and my siblings Faizal, Hafiz, Intan Azira, Razif, Razi, Ellesa, and Fahmi's endless love, prayers, understanding, patience, financial support, and encouragement, I would not have been able to concentrate and accomplish my objectives. Allah bless you everyone for the little ways in which you have helped me.

During the course of my research, I would like to thank the members of CFD Group for sharing their academic knowledge, friendship, and cooperation with me. I owe them for their assistance on my trip. Without the aid of the above-mentioned persons, it is probable that I will be unable to finish my thesis and will have tremendous difficulties throughout its completion. The assistance and recommendations greatly aided the completion of my task. I am grateful for all the help and assistance during my thesis.

ABSTRAK

Kajian terhadap kesan aliran angin di sekeliling rumah bertingkat rendah dengan jenis bumbung bersudut tunggal yang melibatkan juntaian bumbung menjadi fokus di dalam kajian ini. Banyak angin ribut berlaku sejak beberapa bulan ini dan menyebabkan kerosakan pada bumbung terutamanya yang melibatkan rumah bertingkat rendah. Walaubagimanapun, kajian-kajian lepas terhad kepada rumah dengan jenis bumbung gabel. Kajian berangka menggunakan simulasi Perkomputeran Dinamik Bendalir dijalankan untuk mensimulasikan aliran angin terhadap rumah bertingkat rendah, seterusnya menghasilkan taburan tekanan di sekeliling rumah. Oleh itu, kajian ini dijalankan untuk mengkaji kesan juntaian dan sudut bumbung di sekeliling rumah bertingkat rendah menggunakan Perkomputeran Dinamik Bendalir. Persamaan RANS menggunakan model bergelora RNG k- ϵ diperkenalkan untuk menyelesaikan masalah aliran dalam kajian ini. Pekali tekanan yang tertinggi di model MR 5 telah direkod ialah 0.97. Sementara itu, model yang bersudut bumbung 18° telah menghasilkan sedutan tertinggi berlaku di juntaian bumbung dengan nilai pekali tekanan, C_p bersih dikira sebanyak -2.6933. Akhir sekali, keputusan dan rekabentuk yang menggunakan juntaian bumbung dan sudut bumbung 18° memberi kesan kuat kepada nilai C_p .

ABSTRACT

The study of effects of wind flow surrounding the low-rise house with mono-pitch roof considering overhang become the focus of the present study. Many windstorms event occur past few months and cause several damaged to the roof especially in low-rise house. However, the previous studies are limited to the low-rise house with gable roof. The numerical study using Computational Fluid Dynamic (CFD) simulation was performed to simulate the wind flow toward house, resulting a pressure distribution surrounding the house. Therefore, the study is conducted to investigate the effect of house features namely overhang and roof pitch on the wind flow surrounding the low-rise house using CFD. The steady-RANS equation using RNG k- ϵ turbulence models were introduced to solve the flow problems for this study. The highest-pressure coefficient was recorded to be 0.97 for model MR 5. Meanwhile the model with 18° roof pitch developed the highest suction effect occurred on the roof overhang with the values of net C_p calculated to be -2.6933. Finally, the results using overhang roof and roof pitch of 18° cause the most significant influences to the C_p values.

TABLE OF CONTENT

	Page
ACKNOWLEDGEMENT	ii
ABSTRAK.....	iii
ABSTRACT	iv
TABLE OF CONTENT	v
LIST OF FIGURES.....	vii
LIST OF TABLES.....	ix
CHAPTER 1 INTRODUCTION	1
1.1 Background of study	1
1.2 Problem statement	4
1.3 Objectives.....	4
1.4 Scope of study	5
1.5 Thesis Organization.....	5
CHAPTER 2 LITERATURE REVIEW	6
2.1 Introduction	6
2.2 Flow characteristics of the building's airflow	7
2.3 Factors affecting the wind induced damages	8
2.4 Factors affecting air flow surrounding the building.....	10
2.5 Computational wind engineering	11
2.6 Turbulence Model	11
2.7 Type of wind test analysis.....	12
2.7.1 Wind tunnel test	12
2.7.2 Computational Fluid Dynamic (CFD)	13
2.8 Summary	15
CHAPTER 3 METHODOLOGY	16
3.1 Introduction	16
3.2 Flowchart for numerical simulation procedures.....	16

3.3	Validation study from previous research study.....	18
3.4	Numerical method for the house model	18
3.4.1	Pre-processing for the house model.....	18
3.4.2	Solving the house model using CFD	25
3.4.3	Post-processing for the house model	27
3.5	Summary of Methodology	30
CHAPTER 4 RESULT AND DISCUSSION		31
4.1	Introduction	31
4.2	Validation results between the previous and current study.....	31
4.3	Numerical simulation of low-rise house using CFD.....	31
4.3.1	Grid sensitivity analysis.....	32
4.3.2	Overall effect around a low-rise house model	36
4.4	Summary of results.....	55
CHAPTER 5 CONCLUSIONS AND RECOMMENDATIONS		56
5.1	Conclusions of research work	56
5.2	Future Recommendations.....	56
REFERENCES		58
APPENDIX A		

LIST OF FIGURES

Figure 1.1 Examples of roof uplift of low-rise house in Ipoh, Perak (The Star,2022). ...	2
Figure 2.1 Wind flow pattern around a low-rise building (Liu, 1991).	7
Figure 2.2 The behaviour of the roof when subjected to the wind loading (Tamura,2009).....	9
Figure 3.1 Flowchart of CFD simulation	17
Figure 3.2 Schematic drawing of MR 15 house model	19
Figure 3.3 The schematic diagram of computational domain and boundary conditions for the house model.....	24
Figure 3.4 Side view meshing of the house model	25
Figure 3.5 The locations of the cut section for overhang 0.75 m	28
Figure 3.6 Net pressure on overhang roof	29
Figure 3.7 Zones designated for each part of the house	30
Figure 4.1 View of grids for grid sensitivity analysis (a) 0.1 mesh; (b) 0.2 mesh (c) 0.3 mesh (d) 0.4 mesh ;(e) 0.5 mesh	35
Figure 4.2 Comparison of pressure coefficient for grid sensitivity analysis	36
Figure 4.3 Pressure coefficient distribution along transverse profile of model FR and model FR OH.	37
Figure 4.4 Streamlines along the transverse profile of the model a) FR OH ; b) FR. ...	39
Figure 4.5 Pressure coefficient distribution along transverse profile of model MR 5 and model FR OH.	41
Figure 4.6 Streamlines along the transverse profile of the model a) FR OH ; b) MR 5	43
Figure 4.7 Pressure coefficient distribution along transverse profile of model MR 10 and model FR OH.	44

Figure 4.8 Streamlines along the transverse profile of the model a) FR OH ; b) MR 10	46
Figure 4.9 Pressure coefficient distribution along transverse profile of model MR 15 and model FR OH	48
Figure 4.10 Streamlines along the transverse profile of the model a) FR OH ; b) MR 15	49
Figure 4.11 Pressure coefficient distribution along transverse profile of model MR 18 and model FR OH	51
Figure 4.12 Streamlines along the transverse profile of the model a) FR OH ; b) MR 18	52
Figure 4.13 Pressure coefficient distribution along transverse profile of all models. ...	54

LIST OF TABLES

Table 3.1 Summary of house development.....	19
Table 3.2 Dimension of the overall models	20
Table 3.3 Input parameters in Ansys FLUENT 14	24
Table 3.4 The properties of air for the turbulence flow	26
Table 4.1 Highest percentage difference of pressure coefficient for model FR based on reference model.....	38
Table 4.2 Highest percentage difference of pressure coefficient for model MR 5 based on reference model.....	41
Table 4.3 Highest percentage difference of pressure coefficient for model MR 10 based on reference model.....	45
Table 4.4 Highest percentage difference of pressure coefficient for model MR 15 based on reference model.....	48
Table 4.5 Highest percentage difference of pressure coefficient for model MR 18 based on reference model.....	51
Table 4.6 Net pressure on the overhang of the roof.....	54

CHAPTER 1

INTRODUCTION

1.1 Background of study

According to Bachok et al. (2012), windstorms are a natural occurrence for Malaysia. As a result, some regions of Malaysia will experience windstorms annually. Windstorms are regarded as a natural danger resulting from the acceleration of the wind's speed (Goldman et al., 2014). The majority of recent wind-related damages in Malaysia were caused by windstorms. The amount of unexpected windstorms in Malaysia has increased significantly as a result of global climate change. The frequency of windstorms has changed significantly from year to year, and this is especially true from 2000 to 2012 (Bachok et al.,2012). In 2009, 110 windstorms were the highest number ever recorded.

A unusual storm destroyed a considerable number of residences in Taman Tasek Damai and Kampung Tawas. During the event at 6:40 p.m. on Sunday, roof tiles were blown off and power poles were also downed. Some locals compared the occurrence like being struck by a tornado. Cheah Kim, a canteen worker in her fifties, said that there was just drizzle, but the wind was "extremely powerful." "I saw the roof of my neighbour being blown off. "My own roof and ceiling have collapsed," she stated when she was approached (The Star,2022). Figure 1.1 depicts the low-rise houses in Ipoh, Perak, that sustained substantial damage to their trusses and roofs during a windstorm.



Figure 1.1 Examples of roof uplift of low-rise house in Ipoh, Perak (The Star,2022).

Malaysia has two monsoon seasons each year, the Southwest Monsoon from late May to September and the Northeast Monsoon from October to March. Northeast Monsoon precipitation exceeds that of the Southwest Monsoon. Southwest Monsoon begins in the Australian deserts, whereas Northeast Monsoon begins in China and the north Pacific. During the Northeast Monsoon, winds of 10 to 20 knots from the east or north-east predominate (MMD, 2016). This will have a big effect on the rural sections of Malaysia's northern region, which comprises of wide stretches of open land. This is because rice plantation agriculture is the principal economic activity in these areas. As there are no barriers to break up the wind during the wind flow, the wind will rise. The increasing wind speed will impact the rural area next to the open environment. Consequently, rural dwellings are more prone to be impacted by high winds.

Wind is an irregularly variable, dynamic phenomena comprised of several eddies of varied sizes and spinning features that move relative to the ground. These eddies cause variances and establish a complicated flow pattern, which contributes to the gustiness of the wind. The wind vector at any given place is the sum of the mean wind vector and the fluctuation components. These components vary not just with altitude, but also with the approach's geography and terrain. The dominant wind exerts pressure on the structures' surfaces. The effects of wind pressure in the form of shear and bending moments are

highlighted as a major cause of structural collapse (Nizamani, 2018).

Malaysia is a country located near the equator. It is equally essential to comprehend that two major monsoons impact the Malaysian wind pattern. The maritime exposure of Malaysia is mostly responsible for the country's steady temperature, high humidity, and frequent precipitation. The climate of this nation is almost stable throughout the year. Despite the fact that the wind over Malaysia is normally weak and variable, there are sporadic modifications in the wind flow patterns that are consistent. Two primary monsoons govern the flow pattern of Malaysia's wind system (Ramli et al., 2014).

The wind forces acting on a structure are not constant but rather dynamic and extremely variable. In addition to wind force, pressure fluctuations may cause significant structural damage. The quasi-steady assumption is one method for safely assuming wind pressures, in which the building is considered to be a motionless rigid body in wind and the wind pressure applied to the structure is a constant lateral force. This strategy is suitable only if the building height is below 50 metres (Mendis et al., 2007).

ASCE 7-10 defines low-rise buildings as having an average roof height that is less than the lowest horizontal dimension and less than 18.3 metres. They account for the vast bulk of commercial, residential, and industrial buildings. Ninety percent of current low-rise residential structures are unfinished wood light-frame constructions, making them more susceptible to severe wind pressures, wind-borne debris, and rainfall penetration (Pan, 2014).

As the global climate has altered over the last decade, reports of economic losses caused by tropical cyclones have grown. In 2015, economic losses in the typhoon-prone southeast coast of China totaled \$9.97 billion, and 10,000 buildings were damaged or destroyed (Ma and Wang, 2015). Roof collapses of low-rise residential buildings were the major cause of catastrophic disasters during typhoon landfalls (Uematsu and

Isyumov, 1999). In general, partial or total roof damage during windstorms was identified to be the major failure mechanism of low-rise buildings (Shanmugasundaram et al., 2000).

A violent storm destroyed this village, impacting more than 300 people and leaving a path of ruin in its wake. During the incident around 3 p.m., the strong winds and rain tore the roofs off more than 100 homes in Kampung Tasek, causing massive leaks and floods. (Kaur, 2021). The roof pitch of the core residence for twenty-five damaged homes located near the northern frontier of Peninsular Malaysia ranges from 7° to 27° (Zaini et al., 2017). Additionally, Table 5.3(b) of MS 1553:2002 covers an equivalent 10° to 45° range.

1.2 Problem statement

Wind disasters are responsible for tremendous physical destruction, injury, loss of life and economic damage. The failure of a roofing system during a windstorm maybe resulted from strong wind pressure. In addition, the mono-pitch roof with overhang is not covered in the MS 1553 2002 Code of Practice on Wind Loading for Building Structure. The use of mono-pitch roofs on low rise buildings in Malaysia increases due to its aesthetic value. Hence, this study will focus on the wind analysis of different roof slope and profile of low-rise buildings with mono-pitch roof.

1.3 Objectives

This research is intended to study the effect of roof slope on the wind pressure distribution of a low-rise mono-pitch house is focusing on the following objectives:

1. To evaluate the distribution of pressure coefficient along the profile of a low-rise house with mono-pitch roof.
2. To determine the net pressure acting across the overhang roof

1.4 Scope of study

This work is restricted to the CFD modelling of a low-rise house. This method will be simulated using the ANSYS Fluent 14.0 software. This programme is able to compute the pressure exerted on a house due to wind speed at the building's entrance and a range of ground roughness. The model will be constructed with the data collected by (Abdullah et al., 2019). In this research, a two-dimensional (2D) model of a single-story house will be used, with the incoming flow perpendicular to the roof ridge. This study employs a closed, two-dimensional model that works with flat terrain. The result of this numerical simulation will be assessed in terms of C_p .

1.5 Thesis Organization

This thesis has four more chapters that are ordered as follows:

Chapter 2: Literature Review. This chapter provides a concise overview of housing development in Malaysia. The wind-induced damage and airflow around the structure are caused by the wind-affecting variables. This chapter describes the fundamentals of computational wind engineering and types of wind test analysis.

Chapter 3: Methodology. This chapter discusses the study's general methodology, which includes numerical processes. This chapter describes in detail the numerical study utilising the CFD approach, as well as the pre-processing step, which includes the generation of the model, mesh, computational domain and boundary conditions.

Chapter 4: Results and Discussions. This chapter provides and examines the results of the house model's numerical simulation.

Chapter 5: Conclusions and Recommendations. Before coming to conclusions, this chapter highlights the major results and analyses the aims of the study. In addition, prospects for further study and research are suggested.

CHAPTER 2

LITERATURE REVIEW

2.1 Introduction

Housing is an essential aspect of everyday living not only because of its price, but also because it provides access to other aspects of a good city life. Specifically, housing may help residents cope with the struggle to maintain economic livelihood, the dangers of a changing environment, the issues of urban crime, and government injustices. From 2006 to 2010, there will be a need for 709,400 units of housing in Malaysia. Twenty thousand units are allotted to the very poor, those living below the poverty line, whose housing needs are of paramount concern. Low-income earners own 165,400 units of low-income housing and 85,505 units of affordable housing (Bakhtyar et al., 2013).

Under the Seventh Malaysia Plan, a total of 800,000 housing units were to be erected in Malaysia, while under the Eighth Malaysia Plan, a total of 782,300 housing units were to be built. During the Ninth Malaysia Plan, it is anticipated that 709,400 units of additional housing would be required, of which 19.2% will be in Selangor, 12.9% in Johor, 9.4% in Sarawak, and 8.2% in Perak (Zainun et al., 2010). Therefore, the Ninth Malaysian Plan (9MP) placed significant emphasis on affordable housing. The total performance of houses constructed under the category of low-cost housing is positive, with 200,513 units finished, or 86.4 percent of the goal. 51.5 percent, or 103,219 units, were created by the public sector, which includes state economic development enterprises. To guarantee a sufficient supply of low-cost housing, private developers must commit at least 30 percent of their mixed-development projects to low-cost housing (Bakhtyar et al., 2013).

2.2 Flow characteristics of the building's airflow

Figure 2.1 shows how the air moves around a model of a low-rise building when the wind is coming from the front (Liu, 1991). The airflow split at the corner of the windward wall and the leading roof. The place where the two things split up is called the separation point. Because of the earth and the windward wall in this spot, a recirculation zone was made. The area where air flows back and forth is often called a "standing vortex" (Kutter et al., 2017). Holmes (2007) found that there was a point on the surface of the windward wall where the speed of the wind coming in stopped. Tominaga et al. (2015) said that under normal conditions, the stagnation point was at about two-thirds of the height of the windward wall.

As the flow gets closer to the ridge on the windward side, backflow creates a separation zone on the surface of the roof. Most of the time, the air pressure in the separation zone is lower than the pressure in the surrounding area. This causes changes in suction. Behind the leeward wall, a wake or vortex forms, which is a pocket of flow that forms behind a structure. This makes the surfaces in this area pull together.

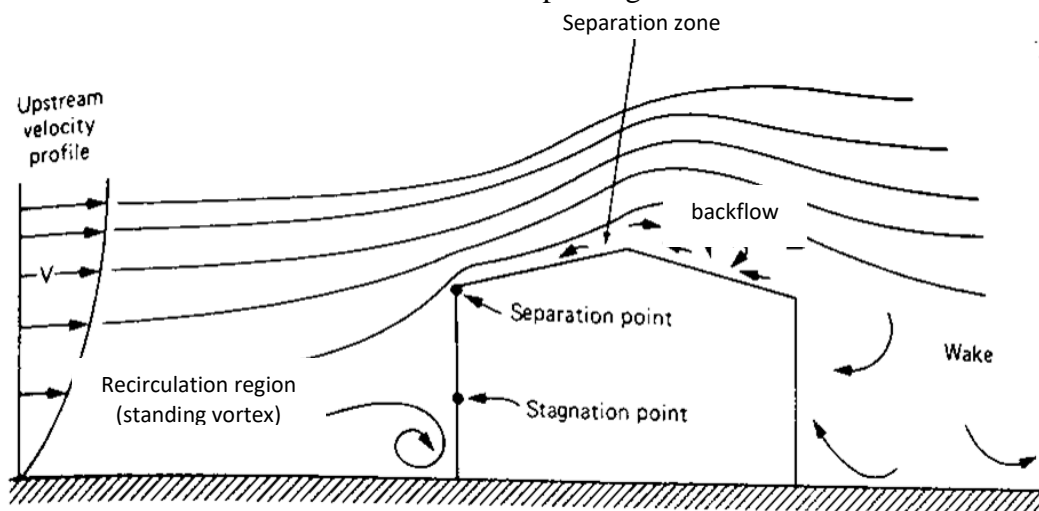


Figure 2.1 Wind flow pattern around a low-rise building (Liu, 1991).

2.3 Factors affecting the wind induced damages

According to Tamura (2009), several phenomena affect structures and their environments under heavy winds, occasionally leading to their collapse. It should be emphasised that damage relies not only on wind speed, but also on the strength or quality of buildings and that the phenomena listed in the table might result in varying degrees of destruction.. Roof damage happens either directly or indirectly as a result of apertures being broken. The majority of damage to roofs occurs as a result of localized high suctions and substantial pressure changes at the roof's perimeter and projecting parts. As seen in Figure 2.2, these small failures let wind to penetrate under the roof parts, raising the beneath pressure and quickly increasing lift forces. Thus, little roof damage might result in the complete disintegration of the roof. Complete roof lift-off may also be caused by damage to apertures such as glass windows, which allows wind into the space and increases the pressure underneath.

A breach in an aperture causes either direct or indirect harm to the roof. The bulk of roof damage is caused by localized high suction and significant pressure fluctuations near the roof's perimeter and protrusions. As seen in Figure 2.2, these minor failures allow wind to infiltrate under the roof components, hence rapidly increasing lift forces. Consequently, little roof damage might lead to the full collapse of the roof. Damage to openings such as glass windows may potentially lead to a complete roof lift-off by allowing wind into the area and increasing the pressure beneath (Tamura, 2009).

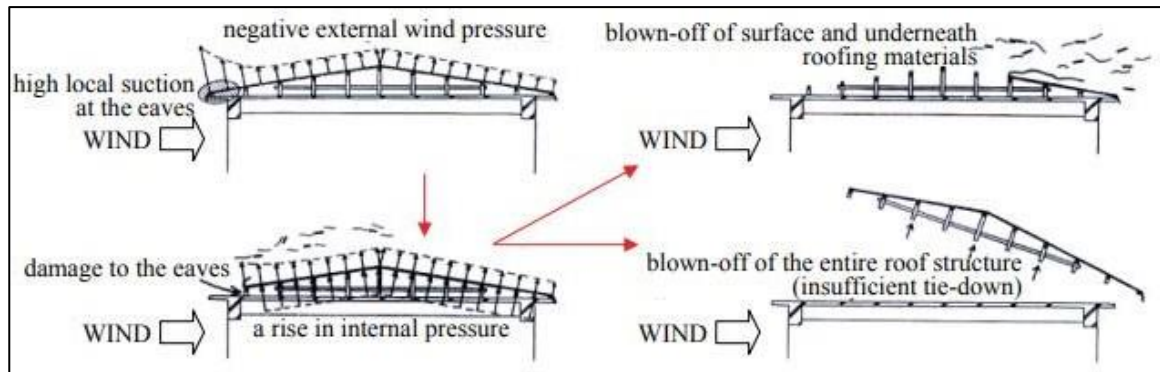


Figure 2.2 The behaviour of the roof when subjected to the wind loading (Tamura,2009)

At the eaves of gable roofs, as well as the ridges and corners of hipped roofs, there have been many cases of clay tiles partly detaching. The vast majority of roof tile installation is performed using nails and steel wires throughout the whole perimeter of the roof, including the eaves and ridge. However, lift-off of non-fixed shingles also occurs in the centre of roofs. Damage to tile roofs rises when the substrate is simplified, i.e., when the weight is decreased by eliminating the roofing cement, resulting in the formation of gaps between the substrate and the tiles. Once an unfixed tile in the centre part is lifted, wind may enter the region underneath, causing successive tile lift-off. Negative pressure and substantial turbulence cause the tiles on the leeward side of a hipped roof to peel off (Tamura, 2009).

If nails and steel wire are not effectively protected against rust, they lose their strength and are unable to fulfil their intended function within a few years. Important countermeasures include securing roof sheathing boards to the whole roof area, including the centre, and filling gaps with lime plaster. It is suggested to do inspections every 5–6 years and to replace every 20–30 years (Tamura, 2009).

2.4 Factors affecting air flow surrounding the building

In a study on community housing design requirements for severe events, it was discovered that the deterioration of the cladding is often the earliest indication of building collapse and resident damage (Coulbourne et al., 2002). The vulnerability analysis of a study of wind load on roof shingles revealed that the net wind uplift loading on tiles, as opposed to exterior surface forces, enhanced tile disintegration (Li et al., 2014). Therefore, wind load must be addressed with other loads while building the structure. High wind-induced suctions may cause substantial damage to outdated roofing systems, resulting in water ingress and material loss.

When a structure is hit by wind load, the wind load is mostly made up of drag force and lift force, both of which can be positive or negative wind pressures. A research of tension leg platform superstructures discovered that drag force increased in surge and heave responses, despite the fact that the impact of current drag is often governed by the magnitude of the wave energy spectrum (Oyejobi et al., 2016). Extreme wind conditions cause a number of losses, such as broken window frames and glass and damage to the building envelope, which lets water into the building.

The design of nearby structures, the height of nearby buildings, and the distance between nearby buildings and the main structure all have a big effect on the wind load on the main structure. Changes in the distance between two opposing walls caused a big change in the pressure coefficients of the structure, which may be caused by shielding. This suggests that having structures next to each other doesn't always make the wind pressure on the central structure lower. The direction of the wind also has a big effect on how much pressure there is. The wind load on a building is equal to the square of the speed of the wind (Sarkar et al., 2014).

Numerous studies have been undertaken on the variables that affect wind flow around

low-rise homes, such as overhang, roof pitch, roof geometry interference, and surroundings. Multiple variables hindered the estimation of wind load on low-rise structures (Irtaza et al., 2015). One of them is the interference effect, which is often caused by things like nearby buildings, structures, free-standing walls, groups of buildings, and trees that block the signal. These obstructions will cause changes in wind pressure, streamline deflection, local circulation patterns, suction and stagnation pressure, and suction and stagnation pressure. Low-rise buildings are often surrounded by many obstacles, whether they are in an urban or rural area. Most of the metropolitan area is surrounded by houses and other buildings.

2.5 Computational wind engineering

Computational Wind Engineering (CWE) is one of the most extensively used methodologies in wind engineering for tackling wind engineering challenges, according to (Franke et al., 2004) and others (Blocken, 2014). CWE is often defined as the wind engineering application of CFD. Despite this, CFD models may be able to address wind-related issues faster and at a lower cost than wind tunnel testing (Zhang et al., 2005).

The American Society of Civil Engineers says that CFD can be used to analyse and design buildings in many ways, such as measuring air flow, the wind around buildings, ventilation of structures, and wind-driven rain on building faces (Blocken, 2014). CFD is also used to figure out how buildings and the people in and around them will be affected by wind (Palmer et al., 2003).

2.6 Turbulence Model

CFD turbulence models used in engineering include Reynolds-averaged Navier-Stokes (RANS) models and Large-Eddy Simulation (LES) models (Tominaga, 2015). Franke et al. (2007) asserted that the RANS equations adequately capture the wind tunnel experiment since the average flow conditions inside the tunnel do not vary over time.

This reduces the time necessary to do the computations. On the other hand, the LES model tries to be more accurate and show transient wind circulation on the leeward side of the buildings, but it takes a lot more time. This model is widely used in engineering since it is based on the Reynolds averaged equations and has a solid reputation for precision. It seems to be the most competent model for current applications to address a wide range of wind engineering issues (Murakami,1990).

2.7 Type of wind test analysis

2.7.1 Wind tunnel test

In a wind tunnel study, it was found that the wind pressure on different parts of a "+"-shaped structure can change depending on how the wind hits it (Chakraborty et al., 2014). Wind tunnel testing or wall of wind (WOW) studies can be done to figure out a building's wind load, but they take a long time, cost a lot of money, and require a lot of work. Also, there isn't enough equipment for experiments, like wind tunnels and wind-on-water (WOW) systems. So, there needs to be an alternative to experimental investigation to make up for all of its flaws. At the moment, CFD models or numerical analysis can be used instead of experimental research to control how wind loads affect structures (Roy et al, 2017).

Experiments in a wind tunnel are expensive and take a long time, and they can't be used to measure Reynolds numbers at full scale (Re). The turbulence and boundary layer of the atmosphere may also be harder to simulate in places with complicated landscapes. In some ways, numerical wind load prediction is better than scale models in boundary layer wind tunnels. For example, any Reynolds number, turbulence, and boundary layer profile can be simulated. With a numerical technique, it's also easy to do parametric studies because it's easy to change the boundary conditions. So, numerical simulations have a lot of potential to improve rules of conduct. The choice of appropriate boundary conditions,

discretization methods, and, most importantly, turbulence models is very important to the accuracy of predictions. During the last 40 years, many scientists have made important contributions to computational wind engineering.

Mathews (1987) states that computers are used to assess wind-generated pressure patterns around structures. These pressure patterns were crucial in predicting the natural ventilation of buildings. It was determined that the projected distribution of pressure was accurate. Mathews and Mayer (1987) said that accurate modelling of wind loads on greenhouses is necessary for their secure construction. Wind loads on a semicircular greenhouse have been estimated numerically. In addition, parametric analyses of the effects of Reynolds number and terrain roughness on the wind-induced pressure distribution around the greenhouse were presented.

A comparison was made between the pressure distribution at high Reynolds numbers and published full-scale data. Baskaran and Stathopoulos (1989) conducted computer evaluations of the impact of wind on structures. Using three-dimensional turbulent flow conditions, a computer simulation of wind flow around a cube-shaped structure was tried. For numerical discretization, the Control Volume Method was applied. The pertinent extensive literature review on the numerical prediction of wind loads using the RANS (Reynolds Average Navier-Stokes) model, the Large Eddy Simulation (LES) model and the model is available elsewhere (Zaheer, 2007).

2.7.2 Computational Fluid Dynamic (CFD)

In computational fluid dynamics, often known as CFD, numerical analysis is used to provide solutions for various fluid flow-related problems (Blocken et al., 2008). CFD is a numerical technique that may be used to both two- and three-dimensional scenarios. Alternative numerical analytic approaches exist for 2D, 3D, and 4D problems, such as hybrid orthonormal Bernstein, block-pulse functions wavelet method, time-fractional

Benjamin-Ono (BO) equation, Boiti– Leon–Manna–Pimpinella equation, and Haar wavelet method (Ali, 2019). Consequently, CFD is defined as the assessment of fluid flow behaviour utilising applied mathematics, physics, and computer software (Rouse,2014). As a result, numerical simulation is used in the present study.

CFD modelling is a versatile and very beneficial approach (Blocken, 2014) and is therefore ideal for studying the unstable aerodynamic loads on the vibrating roofs in a larger, lower frequency range (Ding et al., 2014). CFD reduces both the time and cost of design and research while providing rich, visual data (Canonsburg, 2013). Wind tunnel testing is one approach for examining the wind loading of structures, although it is difficult, time-consuming, and expensive. In this study, the wind load analysis for a pyramidal roof on a low-rise building with a square plan was performed using CFD modelling and simulation (Singh and Roy., 2019).

In design and research, CFD decreases cost and time and gives visible and complete data (Canonsburg, 2013), and ANSYS Fluent has been used for a number of wind load studies (Hoof et al., 2015). This application is user-friendly without sacrificing accuracy or speed (Kuzmin, 2018). Also, throughout the last half-century, CFD has become an important research tool for structural aerodynamics (Blocken., 2014). As an alternative to wind tunnel experiments, a substantial number of research inquiries have been undertaken using CFD modelling, and the CFD results have shown outstanding agreement with the experimental results (Blocken et al., 2007).

For the simulation of geometric models like SST, LES, and k- ϵ . This study requires a CFD analysis because the evaluation of the performance of the different roof geometries is dependent not only on the pitch of the roof surface and wind direction, but also on the airflow pattern (velocities) around the building as a result of the different vertical exposed area. CFD has been a strong tool for study in urban physics and building aerodynamics

during the last 50 years (Blocken, 2014). The compressible stable Reynolds-Averaged Navier Stokes (RANS) equations were solved using the finite volume approach based Open Foam solver (Li et al., 2006). Various turbulence models are utilised to identify the model that best replicates the findings of both the full-scale and wind tunnel measurements of the wall-mounted cubic bluff body (Irtaza et al., 2013).

2.8 Summary

The majority of research to date have been conducted on low-rise structures with gable roofs, hip roofs, multi-span gable roofs, canopy roofs, sawtooth roofs, monoslope roofs, and dome-shaped roofs. Therefore, research on mono-pitched roof with overhang structures is quite restricted to date. As previously indicated, prior research has been conducted on other types of roofs and the wind standards of various countries provide wind pressure coefficient values for several roof forms other than mono-pitched roofs and few earlier research indicate that the air flow characteristics around these houses alter as a consequence of the kitchen's existence. In addition, another study examined the air flow characteristics along the 2-D profile of a rural house model situated a top a ridge terrain, taking into account the influence of modifying the terrain height (Abdullah et al., 2019). The research was also performed with the Computational Fluid Dynamics approach included into the ANSYS Fluent software suite. CFD simulation is used in the current work to explore the influence of roof pitch on the wind pressure distribution of a low-rise mono-pitch house.

CHAPTER 3

METHODOLOGY

3.1 Introduction

This section explains the numerical methods required to perform a CFD analysis using ANSYS Fluent 14. Using ANSYS Design Modeler, the model was built. Computational fluid dynamics is a useful technique for calculating the pressure distribution. The approaches started with the collection of essential data and the validation of the $k-\epsilon$ turbulence model (Abdullah et al., 2019). In addition, the field data gathered from the previous research done by (Zaini et al., 2017). Next, the CFD simulation numerical simulation techniques in ANSYS Fluent 14.0 are detailed in detail. Lastly, the method for detecting the interaction and primary effect of many input components is outlined. Figure 3.1 depicts the methodological flowchart for the whole investigation in accordance with its purpose.

3.2 Flowchart for numerical simulation procedures

In this work, ANSYS Corporation's ANSYS Fluent 14.0 software was used for the CFD simulation. Fluent is one of the ANSYS Workbench apps that focuses on supplying an extensive range of turbulence correctly and effectively (Fluent, 2018). These CFD simulation techniques begin with pre-processing, solution, and post-processing utilising two commercial tools, ANSYS Fluent 14.0 and Tecplot 360. In addition, the grid sensitivity analysis was performed for five distinct grid schemes ranging from 0.1 to 0.5. The model with a grid scheme that satisfies the y^+ (for wall function) criteria has been discovered and parametric experiments have been conducted using the knowledge obtained from previous research.

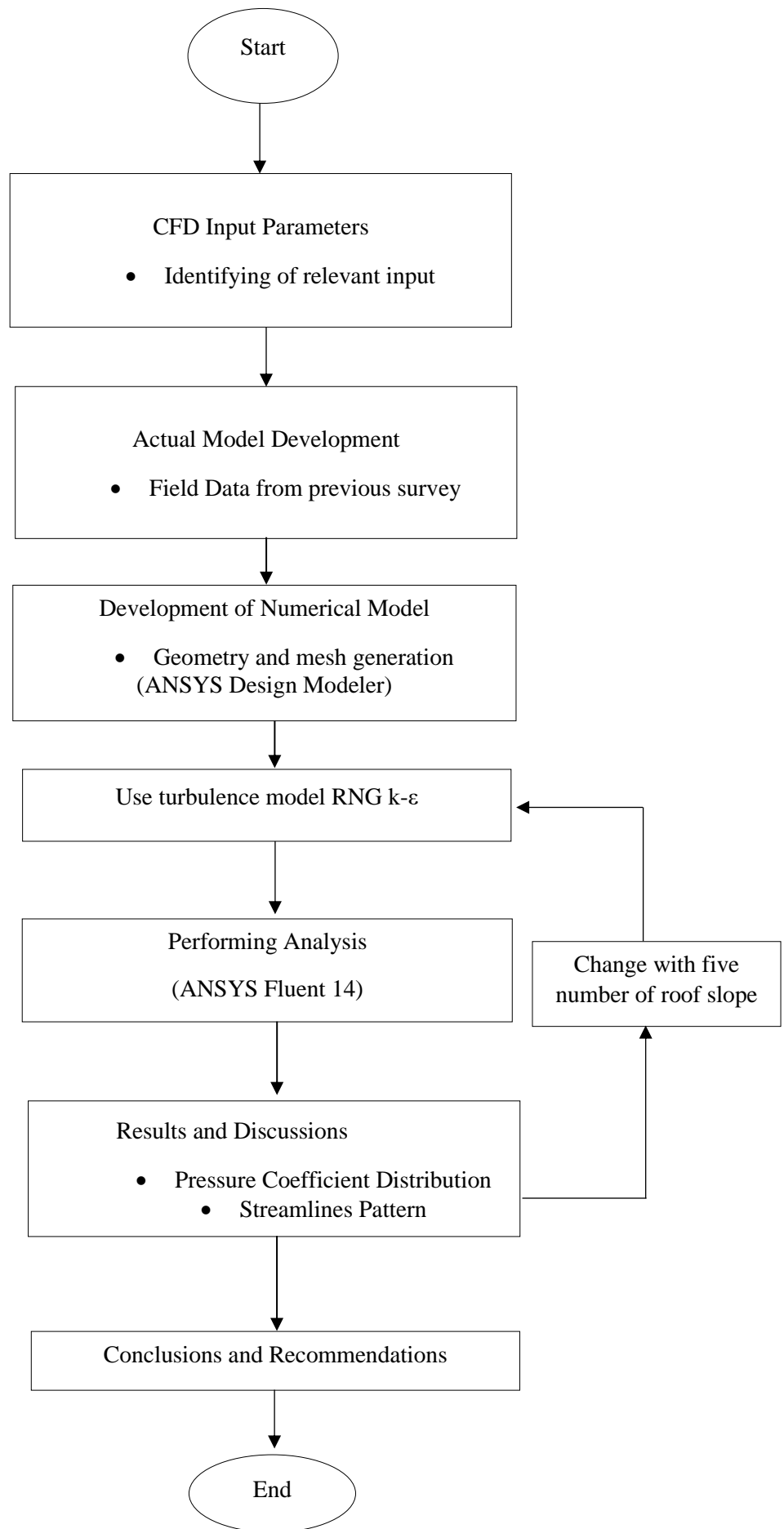


Figure 3.1 Flowchart of CFD simulation

3.3 Validation study from previous research study

In this research, the User Define Function (UDF) from Abdullah et al., (2019) was utilised for validation reasons. The sole correlated parameter is the building's height; the height of the house $H=4\text{m}$ is consistently utilised as in prior research.

3.4 Numerical method for the house model

This section explains the development of the low-rise house model and the methods for applying the mean velocity field with incompressible and viscous turbulent flow based on stable Reynolds-averaged Navier–Stokes (RANS). According to Symscape (2012), a steady-state flow is deemed to exist when all residual graphs settle at or below 1×10^{-3} with increasing iterations. The wind flow was thought to be incompressible due to the constant density of fluids inside a fluid as it flows.

3.4.1 Pre-processing for the house model

This step requires the development of the house's geometric model, including the computational domain, boundary conditions, and grid generation, using an ANSYS tool comparable to AutoCAD to create the computational domain, boundary conditions, and grid. The computational domain, boundary conditions, and grid generation for the house model were equivalent to field information obtained on-site (Zaini et al, 2017).

3.4.1.(a) Development of geometric model for house model

These models were created and adapted from houses in the Peninsula Malaysia area. The house's height was determined to be 4 m. The model was positioned inside the surface boundary layer perpendicular to the oncoming flow. Using the normalising method described by Zaini et al (2017) the dimensions of the house model, including width and height, were fixed to be in the ratio 2:1. At this point, the roof overhang and roof pitch of the house were integrated into the model. The models were built with various roof

itches, as described in Table 3.1.

Table 3.1 Summary of house development.

Parameters	House
House dimension	8 m (W) x 4 m (H)
Overhang (OH)	0.75 m
Roof Pitch (RP)	0°, 5°, 10°, 15° and 18°
Terrain Category	Flat terrain

The model of the house is generated in the design modeler of ANSYS Fluent 14 software. The model dimension that has been determined are the width and height of 8 m and 4 m, respectively. The schematic drawing of the house model without overhang is shown in Figure 3.2 and the details dimension of the overall models is shown in Table 3.2.

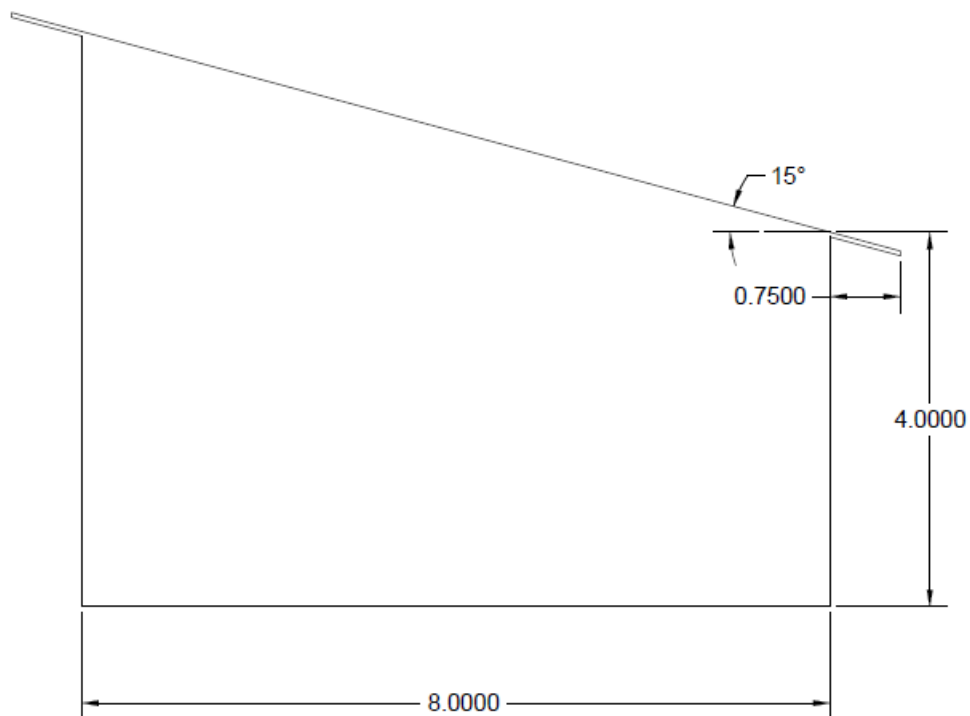


Figure 3.2 Schematic drawing of MR 15 house model

Table 3.2 Dimension of the overall models

House Models	Width (m)	Height (m)	Slope angle	Overhang Length (m)
FR	8	4	0	0.75
FR OH	8	4	0	0.75
MR 5	8	4	5	0.75
MR 10	8	4	10	0.75
MR 15	8	4	15	0.75
MR 18	8	4	18	0.75

3.4.1.(b) Computational domain and boundary conditions for house model

At the model's inlet boundary condition, a fully developed turbulent flow was formed and the vertical wind profile was established as the velocity inlet using the power law equation mentioned in Equation 3.4 as recommended by Liu (1991). Similarly, Equation 3.1 was used to determine the new friction velocity to be integrated into Equations 3.2 and 3.3. Equations 3.2, 3.3, and 3.4 were then translated to UDF and applied to the inflow. The UDF's specifics are included in Appendix A. Tominaga et al. (2015) also utilised a similar method (Zhang, 2009).

Friction velocity, U_o

$$U = \frac{U_o}{k} \ln\left(\frac{Z_{ref}}{Z_o}\right) \quad \text{Equation 3.1}$$

Where,

U = wind velocity (m/s)

U_o = friction velocity (m/s)

k = Von Karman constant with the value of 0.04

Z_{ref} = reference height (m)

z_0 = roughness length of the terrain (m) u^2

Turbulent kinetic energy profile, k :

$$k = \frac{u_o^2}{\sqrt{C\mu}} \quad \text{Equation 3.2}$$

Where,

k = Turbulent kinetic energy (m^2/s^2)

u_o = friction velocity (m/s)

$C\mu$ = Kolmogorov constant with the value of 0.09

Turbulent dissipation rate, ε :

$$\varepsilon = \frac{u_o^2}{k(z+z_o)} \quad \text{Equation 3.3}$$

Where,

ε = turbulent dissipation rate (m^2/s^2)

u_o = friction velocity (m/s)

z = height (m)

Z_0 = roughness length of the terrain (m)

k = Von Karman constant with the value of 0.04

$$V_z = V_{zref} \left(\frac{z}{z_{ref}}\right)^\alpha \quad \text{Equation 3.4}$$

Where,

V_z = wind velocity at height z

V_{zref} = the wind velocity at reference height

z = the height above the ground

z_{ref} = reference height (building height)

α = power-law exponent based on terrain roughness

This model's reference height was also taken into account for the house's height (H). According to Liu (1991), the value of α was set to 1/7, representing exposure type C (open terrain), and the value of roughness length, Z_o , was set to 0.035 metres. In line with Tominaga (2015) and Tominaga et al. (2015), the pressure outlet for the outlet boundary condition was constructed as a pressure-free outlet. The symmetry boundary requirements for the lateral and upper domains were fixed to represent zero normal velocity and zero gradients at all borders, as required by Tominaga et al. (2015).

Additionally, boundary constraints at the bottom of the computational domain were established. As recommended by Franke et al. (2007) and Zhang (2009) the bottom surface of the domain was established as a no-slip wall for wall shear conditions. Roughness height, K_s , and roughness constant, C_s , are crucial factors for the input at the intake. C_s is between 0 and 1 (Fluent, 2010). According to Hargreaves and Wright (2007), Zhang (2009), and Lopes et al. (2010), the relationship between sand grain

roughness height, K_s , and wind flow aerodynamic roughness length, Z_0 is entirely different. However, Blocken et al. (2007a) and Zhang (2009) concluded that roughness length was used directly to obtain better flow and to eliminate the coarse mesh limitation after conducting several experiments.

For this study, implementing the roughness height, K_s as the equivalent sand grain roughness was considered in order to fulfill the limitation of the third requirement. The value of K_s was calculated using the following equation as stated by Blocken et al (2007a). Hargreaves and Wright (2007), Zhang (2009) and Lopes et al. (2010):

$$K_s = \frac{\varepsilon Z_0}{C_s} \quad \text{Equation 3.5}$$

Where,

K_s = roughness height (m)

ε = empirical constant with the value of 9.793

Z_0 = roughness length (m)

C_s = roughness constant

The lateral domain was defined as the 15H distance measured from the inlet and outflow to the end of the rising slope. 15 H was utilised as the clearance height for the top boundary condition. H represents the building model's height, and the home model selected H=4m. The computational domain adheres to the advice provided by Shirasawa et al. (2003) and Mochida et al. (2008). These dimensions were chosen to prevent flow development obstructions. In accordance with Tominaga et al. (2008) advices the blockage ratio was determined to be between 0.85% to 0.955% (less than 3%). The

roughness height (K_s) and roughness Constant (C_s) were subsequently set to 0.035 metres and 1.0, respectively. The wall boundary conditions were added to the home model surfaces as no-slip conditions (zero velocity). The computational domain and boundary conditions for the home model are shown in Figure 3.1.

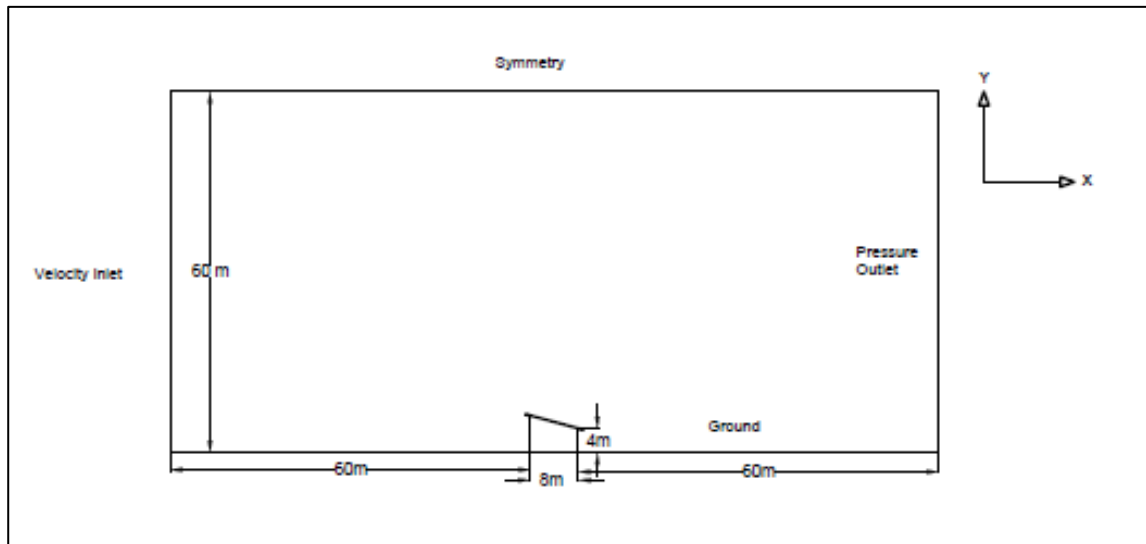


Figure 3.3 The schematic diagram of computational domain and boundary conditions for the house model.

Table 3.3 Input parameters in Ansys FLUENT 14

Item	Data
Computational Domain	128 m x 60 m
Turbulence model	RNG k- ϵ
Near wall treatment	Standard wall function
Power law profile	0.25
Roughness length, Z_0	0.035 m
Roughness height, K_s	0.035 m
Roughness constant, C_s	0.5
Power law profile, α	1/7
Pressure velocity coupling	Scheme (SIMPLE)
Spatial discretization	Gradient (Least square based) Pressure (Second order) Momentum (Second-order)